arXiv:astro-ph/9703117v1 18 Mar 1997

Variable Timestep Integrators for Long-Term Orbital Integrations[1]

Man Hoi Lee and Martin J. Duncan

Department of Physics, Queen's University, Kingston, ON K7L 3N6, Canada

Harold F. Levison

Space Science Department, Southwest Research Institute, Boulder, CO 80302, USA

Abstract. Symplectic integration algorithms have become popular in recent years in long-term orbital integrations because these algorithms enforce certain conservation laws that are intrinsic to Hamiltonian systems. For problems with large variations in timescale, it is desirable to use a variable timestep. However, naively varying the timestep destroys the desirable properties of symplectic integrators. We discuss briefly the idea that choosing the timestep in a time symmetric manner can improve the performance of variable timestep integrators. Then we present a symplectic integrator which is based on decomposing the force into components and applying the component forces with different timesteps. This multiple timescale symplectic integrator has all the desirable properties of the constant timestep symplectic integrators.

1. Symplectic Integrators

Long-term numerical integrations play an important role in our understanding of the dynamical evolution of many astrophysical systems (see, e.g., Duncan, these proceedings, for a review of solar-system integrations). An essential tool for long-term integrations is a fast and accurate integration algorithm. Symplectic integration algorithms (SIAs) have become popular in recent years because the Newtonian gravitational N-body problem is a Hamiltonian problem and SIAs enforce certain conservation laws that are intrinsic to Hamiltonian systems (see Sanz-Serna & Calvo 1994 for a general introduction to SIAs).

For an autonomous Hamiltonian system, the equations of motion are

$$d\boldsymbol{w}/dt = \{\boldsymbol{w}, H\}, \tag{1}$$

where $H(\boldsymbol{w})$ is the explicitly time-independent Hamiltonian, $\boldsymbol{w} = (\boldsymbol{q}, \boldsymbol{p})$ are the $2d$ canonical phase-space coordinates, $\{\ ,\ \}$ is the Poisson bracket, and $d(= 3N)$

[1]To appear in Computational Astrophysics, Proc. 12th Kingston Meeting, ed. D. A. Clarke & M. J. West (San Francisco: Astronomical Society of the Pacific).

is the number of degrees of freedom. The formal solution of Eq.(1) is

$$\boldsymbol{w}(t) = \exp(t\{\ , H\})\boldsymbol{w}(0). \tag{2}$$

If the Hamiltonian H has the form $H_A + H_B$, where H_A and H_B are separately integrable, we can devise a SIA of constant timestep τ by approximating $\exp(\tau\{\ , H\})$ as a composition of terms like $\exp(\tau\{\ , H_A\})$ and $\exp(\tau\{\ , H_B\})$. For example, a second-order SIA is

$$\exp(\frac{\tau}{2}\{\ , H_A\})\exp(\tau\{\ , H_B\})\exp(\frac{\tau}{2}\{\ , H_A\}). \tag{3}$$

For the gravitational N-body problem, we can write $H = T(\boldsymbol{p}) + V(\boldsymbol{q})$, where $T(\boldsymbol{p})$ and $V(\boldsymbol{q})$ are the kinetic and potential energies. Then the second-order SIA Eq.(3) becomes

$$\boldsymbol{p}_{n+\frac{1}{2}} = \boldsymbol{p}_n + \frac{\tau}{2}\boldsymbol{F}(\boldsymbol{q}_n), \quad \boldsymbol{q}_{n+1} = \boldsymbol{q}_n + \tau\boldsymbol{v}(\boldsymbol{p}_{n+\frac{1}{2}}), \quad \boldsymbol{p}_{n+1} = \boldsymbol{p}_{n+\frac{1}{2}} + \frac{\tau}{2}\boldsymbol{F}(\boldsymbol{q}_{n+1}), \tag{4}$$

where $\boldsymbol{F} = -\partial V/\partial \boldsymbol{q}$ and $\boldsymbol{v} = \partial T/\partial \boldsymbol{p}$; this is the familiar leapfrog integrator. For solar-system type integrations, a central body (the Sun) is much more massive than the other bodies in the system, and it is better to write $H = H_{\rm Kep} + H_{\rm int}$, where $H_{\rm Kep}$ is the part of the Hamiltonian that describes the Keplerian motion of the bodies around the central body and $H_{\rm int}$ is the part that describes the perturbation of the bodies on one another. Symplectic integrators using this decomposition of the Hamiltonian were introduced by Wisdom & Holman (1991), and they are commonly called mixed variable symplectic (MVS) integrators.

The constant timestep SIAs have the following desirable properties:
(1) As their names imply, SIAs are symplectic, i.e., they preserve $d\boldsymbol{p} \wedge d\boldsymbol{q}$.
(2) For sufficiently small τ, SIAs solve almost exactly a nearby "surrogate" autonomous Hamiltonian problem with $\tilde{H} = H + H_{\rm err}$. For example, the second-order SIA in Eq.(3) has

$$H_{\rm err} = \frac{\tau^2}{12}\{\{H_A, H_B\}, H_B + \frac{1}{2}H_A\} + O(\tau^4). \tag{5}$$

Consequently, we expect that the energy error is bounded and the position (or phase) error grows linearly.
(3) Many SIAs (e.g., Eq.[3]) are time reversible. Note, however, that there are algorithms that are symplectic but not reversible.

Fig. 1 shows the energy error $\Delta E/E$ of an integration of the $e = 0.5$ Kepler orbit using the constant timestep leapfrog integrator Eq.(4). (In this and all subsequent Figures, the orbits are initially at the apocenter $r_a = a(1+e)$, where a and e are the semi-major axis and eccentricity.) Fig. 1 illustrates that there is no secular drift in $\Delta E/E$.

2. Simple Variable Timestep

For problems with large variations in timescale (due to close encounters or high eccentricities), it is desirable to use a variable timestep. A common practice

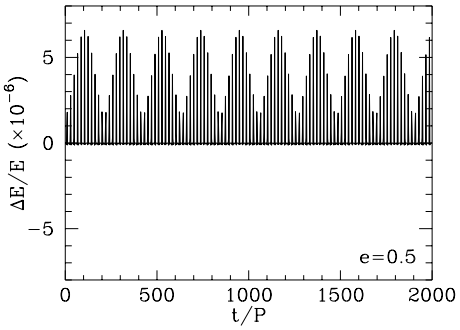


Figure 1. Energy error $\Delta E/E$ of an integration of the Kepler problem using the constant timestep leapfrog integrator Eq.(4). The eccentricity $e = 0.5$, the timestep $\tau = P/4000$, and P is the orbital period.

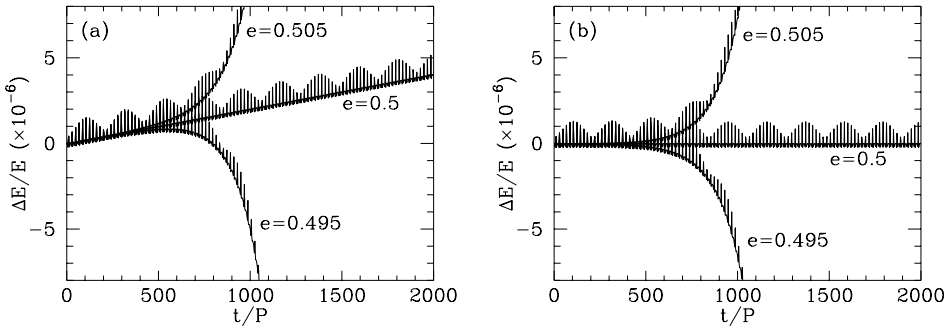


Figure 2. (a) Same as Fig. 1, but using the leapfrog integrator Eq.(4) with the simple variable timestep $\tau = \tau_0(r/r_a)^{3/2}$, where $\tau_0 = P/2000$. The errors for two neighboring initial conditions are also shown (see text). (b) Same as (a), but using the symmetrized timestep criterion.

is to set the timestep using the phase-space coordinates $\boldsymbol{w}_n$ at the beginning of the timestep: $\tau = h(\boldsymbol{w}_n)$. If the SIAs discussed in § 1 are implemented with this simple variable timestep scheme, they are still symplectic if we assume that the sequence of timesteps determined for a particular initial condition are also used to integrate neighboring initial conditions (see Skeel & Gear 1992 for another point of view). However, tests have shown that this and similar simple variable timestep schemes [and also $\tau = h(t)$] destroy the desirable properties of the integrators (e.g., Gladman, Duncan, & Candy 1991; Calvo & Sanz-Serna 1993). In Fig. 2a we show the energy error of an integration with $e = 0.5$ and $h(r) = \tau_0(r/r_a)^{3/2}$. Although the error is initially smaller than that in Fig. 1 (the integrations shown in Figs. 1 and 2 use nearly the same number of timesteps per orbit), it shows a linear drift. In Fig.2a we also show the errors for two neighboring initial conditions ($e = 0.5 \pm 0.005$). They were integrated using the timesteps determined for the $e = 0.5$ orbit. Note that these errors grow even faster.

The degradation in performance is due to the fact that the properties (2) and (3) listed in § 1 are no longer true. The algorithm is not time reversible because the timestep depends only on the coordinates at the beginning of the timestep. Since $H_{\rm err}$ depends explicitly on the timestep τ (see, e.g., Eq.[5]), a variable timestep changes the surrogate Hamiltonian problem that the integrator is solving from step to step. Thus the solution from $t = 0$ to t_n after n steps is not in general the solution of a nearby autonomous Hamiltonian problem.

3. Time Symmetrization

Hut, Makino, & McMillan (1995; see also Funato et al. 1996; Hut, these proceedings) pointed out that the performance of a variable timestep integrator can be improved if time reversibility is restored by choosing the timestep in a time symmetric manner: $\tau = \tau(\boldsymbol{w}_n, \boldsymbol{w}_{n+1})$ with $\tau(\boldsymbol{w}_n, \boldsymbol{w}_{n+1}) = \tau(\boldsymbol{w}_{n+1}, \boldsymbol{w}_n)$. For example, $\tau = [h(\boldsymbol{w}_n) + h(\boldsymbol{w}_{n+1})]/2$. We have tested this idea in detail by (i) integrating a series of problems (the pendulum, Kepler orbits, and the restricted 3-body problem) using a symmetrized variable timestep leapfrog integrator and (ii) integrating the restricted 3-body problem using a symmetrized MVS integrator. We have found that time symmetrization usually reduces the drift in energy (or the Jacobi constant) to negligible levels. Fig. 2*b* shows an integration of the $e = 0.5$ Kepler orbit using the symmetrized leapfrog integrator, and it should be compared to Fig. 2*a*.

In Fig. 2*b* we also show the errors for two neighboring initial conditions that were integrated using the timesteps determined for the $e = 0.5$ orbit. There is no improvement in the error growth for the neighboring initial conditions. Integrating an orbit using the timesteps determined for another orbit may seem to be somewhat artificial, but similar situations do occur in realistic integrations. For example, if we integrate an N-body system using a shared timestep scheme, the timestep used by all of the particles is determined by the few having the strongest close encounter. In practice, since the symmetrized timestep criterion depends on $\boldsymbol{w}_{n+1}$, a symmetrized integrator also has the disadvantage that it requires iteration and can be significantly slower than the original integrator (unless the original integrator is also implicit).

4. Multiple Timescale Symplectic Integrators

In this section we describe a "variable timestep" SIA that has all the desirable properties of the constant timestep SIAs. The algorithm is based on ideas proposed by Skeel & Biesiadecki (1994; see also MacEvoy & Scovel 1994). It is also similar to the individual timestep scheme of Saha & Tremaine (1994).

For simplicity, let us consider in particular the Kepler problem with $T(\boldsymbol{p}) = |\boldsymbol{p}|^2/2$ and $V(\boldsymbol{r}) = -1/r$. We choose a set of cutoff radii $r_1 > r_2 > \cdots$ and decompose the potential V into V_i, or equivalently the force $\boldsymbol{F}$ into $\boldsymbol{F}_i = -\partial V_i/\partial \boldsymbol{r}$, such that (i) $\boldsymbol{F} = \sum_{i=0}^{\infty} \boldsymbol{F}_i$, (ii) $\boldsymbol{F}_i$ (except $\boldsymbol{F}_0$) is zero at $r > r_i$, and (iii) $\boldsymbol{F}_i$ is "softer" than $\boldsymbol{F}_{i+1}$. The force $\boldsymbol{F}_i$ is to be applied with a timestep τ_i. If we assume that $\tau_i/\tau_{i+1} = M_{i+1}$ is an integer, we can apply the second-order SIA in

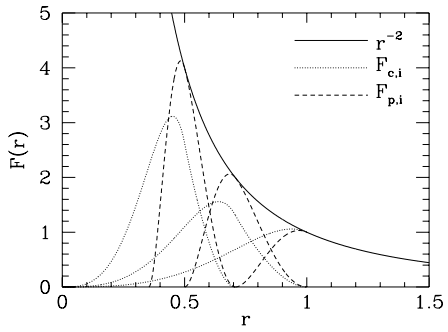


Figure 3. Decomposition of the force $F(r) = 1/r^2$ into $F_{c,i}$ or $F_{p,i}$. The $i = 0$, 1, and 2 components, with $r_1 = 1$ and $r_i/r_{i+1} = \sqrt{2}$, are shown.

Eq.(3) recursively to obtain the following second-order algorithm:

$$\begin{aligned}
\exp(\tau_0\{\ ,H\}) &\approx \exp(\frac{\tau_0}{2}K_0)\ \exp[\tau_0(D+K_1+K_2+\cdots)]\ \exp(\frac{\tau_0}{2}K_0) \\
&\approx \exp(\frac{\tau_0}{2}K_0)\left[\exp(\frac{\tau_1}{2}K_1)\ \exp[\tau_1(D+K_2+K_3+\cdots)]\right. \\
&\qquad \left.\times \exp(\frac{\tau_1}{2}K_1)\right]^{M_1}\ \exp(\frac{\tau_0}{2}K_0) \qquad (6) \\
&\ \ \vdots
\end{aligned}$$

where $D = \{\ ,T\}$ and $K_i = \{\ ,V_i\}$. Hereafter, we adopt $M_i = 2$.

The multiple timescale algorithm Eq.(6) has an overall timestep τ_0, but it is effectively a variable timestep scheme because the recursion terminates at level i if $K_{i+1} + K_{i+2} + \cdots = 0$ during a substep of length τ_i. For example, if the particle is in the region $r_1 > r > r_2$ during an overall step, Eq.(6) reduces to

$$\exp(\frac{\tau_0}{2}K_0 + \frac{\tau_0}{4}K_1)\ \exp(\frac{\tau_0}{2}D)\ \exp(\frac{\tau_0}{2}K_1)\ \exp(\frac{\tau_0}{2}D)\ \exp(\frac{\tau_0}{4}K_1 + \frac{\tau_0}{2}K_0). \quad (7)$$

Since Eq.(6) is based on the recursive application of Eq.(3), it has all the desirable properties of a constant timestep SIA. It is obviously symplectic and time reversible. We can also derive the surrogate autonomous Hamiltonian solved by this integrator. For example, if we decompose V into two levels V_0 and V_1 only, the error Hamiltonian is (cf. Eq.[5])

$$\begin{aligned}
H_{\rm err} &= \frac{\tau_0^2}{12}\{\{V_0,T\},T+\frac{1}{2}V_0\} + \frac{\tau_1^2}{12}\{\{V_1,T\},T+\frac{1}{2}V_1\} + \frac{\tau_0^2}{12}\{\{V_0,T\},V_1\} \\
&\quad + O(\tau_0^4). \qquad (8)
\end{aligned}$$

After some experiments, we found two force decompositions that work well. If we write $\boldsymbol{F}_{c,0} = \tilde{\boldsymbol{F}}_{c,0}$ and $\boldsymbol{F}_{c,i} = \tilde{\boldsymbol{F}}_{c,i} - \tilde{\boldsymbol{F}}_{c,i-1}$ for $i \neq 0$, one of the decompositions is

$$\tilde{\boldsymbol{F}}_{c,i-1} = \begin{cases} -\boldsymbol{r}/r^3 & \text{if } r \geq r_i, \\ -\left[9\,(r/r_i)^2 - 5\,(r/r_i)^6\right]\boldsymbol{r}/4r_i^3 & \text{if } r < r_i. \end{cases} \qquad (9)$$

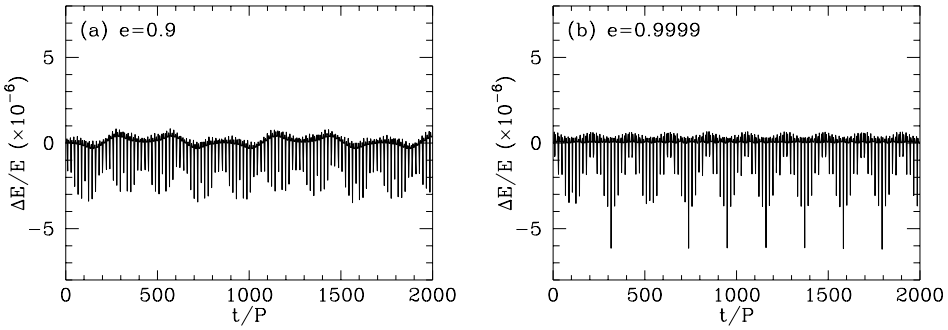


Figure 4. Energy error $\Delta E/E$ of two integrations of the Kepler problem using the multiple timescale symplectic integrator with $\boldsymbol{F}_{c,i}$. The overall timestep $\tau_0 = P/2000$, $M_i = 2$, $r_1 = \sqrt{2}\,a$, and $r_i/r_{i+1} = \sqrt{2}$.

An alternative decomposition uses

$$\tilde{\boldsymbol{F}}_{p,i-1} = \begin{cases} -\boldsymbol{r}/r^3 & \text{if } r \geq r_i, \\ -f\left(\frac{r_i - r}{r_i - r_{i+1}}\right)\boldsymbol{r}/r^3 & \text{if } r_{i+1} \leq r < r_i, \\ 0 & \text{if } r < r_{i+1}, \end{cases} \tag{10}$$

where $f(x) = 2x^3 - 3x^2 + 1$. Unlike the forces suggested by Skeel & Biesiadecki (1994), these forces have continuous first derivatives and decrease rapidly (or exactly) to zero at $r \ll r_i$ (see Fig. 3). We shall not provide the details here, but we can understand why these properties are important from an analysis of $H_{\rm err}$. In Fig. 4 we show the energy error $\Delta E/E$ of two integrations using the multiple timescale symplectic integrator with $\boldsymbol{F}_{c,i}$. As expected, there is no secular drift in $\Delta E/E$. Note also that, with the chosen integration parameters ($\tau_i \propto r_i^2$), the maximum error is almost independent of the pericentric distance (which changes by 10^3 in the two cases shown). This again agrees with the expectation from an analysis of $H_{\rm err}$.

One of the goals of this study is to develop a variable timestep integrator for solar system integrations. We have developed a second-order multiple timescale MVS integrator based on the algorithm described in this section (see Levison & Duncan 1994 for another approach). We are currently testing this integrator in detail. Initial results indicate that the integrator is fast and accurate and has all the desirable properties of the constant timestep symplectic integrators.

References

Calvo, M. P., & Sanz-Serna, J. M. 1993, SIAM J. Sci. Comput., 14, 936

Funato, Y., Hut, P., McMillan, S., & Makino, J. 1996, AJ, 112, 1697

Gladman, B., Duncan, M., & Candy, J. 1991, Celest. Mech. Dynam. Astr., 52, 221

Hut, P., Makino, J., & McMillan, S. 1995, ApJ, 443, L93

Levison, H. F., & Duncan, M. J. 1994, Icarus, 108, 18

MacEvoy, W., & Scovel, J. C. 1994, preprint

Saha, P., & Tremaine, S. 1994, AJ, 108, 1962

Sanz-Serna, J. M., & Calvo, M. P. 1994, Numerical Hamiltonian Problems (London: Chapman & Hall)

Skeel, R. D., & Biesiadecki, J. J. 1994, Ann. Numer. Math., 1, 191

Skeel, R. D., & Gear, C. W. 1992, Physica D, 60, 311

Wisdom, J., & Holman, M. 1991, AJ, 102, 1528